VOC species and emission inventory from vehicles and their SOA formation potentials estimation in Shanghai, China

C. Huang[1*], H. L. Wang[1], L. Li[1], Q. Wang[1], Q. Lu[1], J. A. de Gouw[2], M. Zhou[1], S. A. Jing[1], J. Lu[1], C. H. Chen[1]

1. State Environmental Protection Key Laboratory of the Formation and Prevention of Urban Air Pollution Complex, Shanghai Academy of Environmental Sciences, Shanghai, China

2. Earth System Research Laboratory, Chemical Sciences Division, NOAA, 325 Broadway, Boulder, Colorado 80305, USA

Abstract: Volatile organic compound (VOC) species from vehicle exhaust and gas evaporation were investigated by chassis dynamometer and on-road measurements of 9 gasoline vehicles, 7 diesel vehicles, 5 motorcycles, and 4 gas evaporation samples. The secondary organic aerosol (SOA) mass yields of gasoline, diesel, motorcycle exhausts, and gas evaporation were estimated based on the mixing ratio of measured C2-C12 VOC species and inferred carbon number distributions. High aromatic contents were measured in gasoline exhaust and contributed more SOA yield comparatively. A vehicular emission inventory was compiled based on a local survey of on-road traffic in Shanghai and real-world measurements of vehicle emission factors from previous studies in the cities of China. The inventory-based vehicular organic aerosol (OA) productions to total CO emissions were compared with the observed OA to CO concentrations ($\Delta OA/\Delta CO$) in the urban atmosphere. The results indicate that vehicles dominate the primary organic aerosol (POA) emissions and OA productions, which contributed about 40% and 60% of OA mass in the urban atmosphere of Shanghai. Diesel vehicles, which accounted for less than 20% of vehicle kilometers of travel (VKT), contribute more than 90% of vehicular POA emissions and 80%-90% of OA mass derived by vehicles in urban Shanghai. Gasoline exhaust could be an important source of SOA formation. Tightening the limit of

* Correspondence to C. Huang (huangc@saes.sh.cn)

aromatic content in gasoline fuel will be helpful to reduce its SOA contribution. Intermediate-volatile organic compounds (IVOCs) in vehicle exhausts have great contributions to SOA formation in the urban atmosphere of China. However, more experiments need to be conducted to determine the contributions of IVOCs to OA pollution in China.

Key words: SOA; VOC species; vehicle emission; emission inventory; organic aerosol

1. Introduction

SOA accounts for a significant fraction of ambient tropospheric aerosol (Hallquist et al., 2009; Jimenez et al., 2009). De Gouw and Jimenez (2009) suggested that SOA from urban sources may be the dominant source of organic aerosol globally between 30 and 50 latitude.

Gas-phase oxidation of VOCs has traditionally been considered to be the major source of urban SOA formation. VOCs are oxidized to low vapor pressure reaction products by OH radical, ozone, and NO_3 radical, and eventually form OA in the atmosphere. Odum et al. (1997) investigated the SOA formation from vaporized reformulated gasoline and found single light aromatic hydrocarbons are responsible for the majority of SOA formation. Kleindienst et al. (2002) verified that 75–85% of the SOA was due to reaction products of C6-C9 light aromatic compounds from automobile exhaust. Robinson et al. (2007) further recognized that IVOCs and semi-volatile organic compounds (SVOCs) are also important sources for OA productions based on the smog chamber studies of diesel exhaust and wood fire (Weitkamp et al., 2007; Grieshop et al., 2009). Their subsequent study pointed IVOCs such as long-chain and branched alkanes from vehicle exhaust play more important roles in SOA production compared with other combustion emissions (Jathar et al., 2013). A recent study from Zhao et al. (2014) concluded that primary IVOCs were estimated to produce about 30% of newly formed SOA in the afternoon during CalNex campaign in Pasadena, California.

Due to the abundance of reactive organic compounds, vehicle emission has been recognized as a major source of urban SOA formation (Stone et al., 2009; Liu et al., 2012; Borbon et al., 2013). Laboratory chamber studies also report significant SOA production from diesel, gasoline, and motorcycle exhaust photo-oxidation (Hung et al., 2006; Weitkamp et al., 2007; Chirico et al., 2010; Nordin et al., 2013; Platt et al., 2013). Current research is now focusing on the relative importance of gasoline and diesel vehicles to urban SOA formation. Bahreini et al. (2012) and Hayes et al. (2013) suggested gasoline emissions dominate over diesel in urban SOA formation by field studies. Gentner et al. (2012) argued diesel is responsible for 65% to 90% of vehicular-derived SOA based on the estimation of SOA formation from gasoline and diesel fuel compositions.

Shanghai is one of the most urbanized cities in the Yangtze River Delta (YRD) region in China. The YRD region occupies 2% of land area and generates 8%-12% of the primary $PM_{2.5}$ and the emissions of its precursors in China (Huang et al., 2011). Motor vehicles are the fastest growing source of pollution in the megacities of China. The number of vehicles in Shanghai has doubled in the last decade and reached 2.6 million (about 107 units per 1000 capita) in 2012 (SCCTPI, 2013). Gasoline and diesel vehicles increased by 2.8 and 1.3 times, respectively, while motorcycle decreased by 36%. Vehicular emission has been recognized as the largest source of VOCs in urban Shanghai, which contributes 25%~28% of the measured VOC concentrations. Other VOC emission sources were solvent usage, chemical industry, petrochemical industry, and coal burning, etc. (Cai et al., 2010; Wang et al., 2013). Yuan et al. (2013) indicated that VOC emissions are large contributors to SOA formation through field measurements at a receptor site in eastern China. Huang et al. (2012, 2013) reported that 28.7%-32.1% of the fine particle mass is organic matter (OM) and 30.2%-76% of OM is contributed by SOA in the atmosphere of Shanghai and its surrounding areas. Based on the historical measurement data of organic (OC) and element carbon (EC) in $PM_{2.5}$ in the atmosphere in urban Shanghai, the OC/EC

ratio shows growing trend from 1999 to 2011, which implies that the secondary fraction of organic matter is playing an increasing role in urban Shanghai (Ye et al., 2003; Feng et al., 2005; Hou et al., 2011; Cao et al., 2013; Feng et al., 2013). However, the contribution of VOC emissions to SOA formation and the relative importance of vehicular emission remain unclear. At present, vehicle use is experiencing a rapid growth episode in the cities of China. Understanding the contribution of vehicular VOC emissions to SOA formation will be helpful to identify the source of OA and $PM_{2.5}$ pollution in China.

In this study, we first constructed a vehicular emission inventory of Shanghai for the year of 2012. Then the SOA yields of VOCs emissions from different vehicle types were discussed based on the new measurements of VOCs species from a fleet of vehicles in Shanghai. Finally, we calculated the inventory-based vehicular OA production with the ambient observation data to evaluate the OA contribution of vehicle emission. The main purpose of this study is to discuss: (1) the contribution of vehicle emission to OA in urban Shanghai; (2) the relative contributions of gasoline and diesel vehicles to vehicle derived OA.

2. Materials and methods

2.1 Vehicular emission inventory establishment

2.1.1 Methodology of emission inventory compilation

We developed emission inventories for the pollutants including VOCs, CO, EC, and OC with the IVE (International Vehicle Emission) model for Shanghai, China. The methodology of the model has been introduced by Wang et al. (2008). VKT, vehicle flow distribution, driving pattern, fleet composition and emission factor of each vehicle type were 5 key parameters for the development of vehicle emission inventory. Vehicle emissions can be calculated with Eq. (1).

$$E = \sum_t \left\{ VKT \times f_{[t]} \times EF_{[t]} \times \sum_d \left[f_{[dt]} \times K_{[dt]} \right] \right\} \quad (1)$$

Where, E is emission amount of each vehicle type (g). VKT is Vehicle kilometers of

travel of each vehicle type (km). $f_{[t]}$ is the fleet composition of the specific technology of each vehicle type (%), such as fuel type, engine size, and emission standard. $EF_{[t]}$ is the emission factor of each vehicle technology ($g \cdot km^{-1}$). $f_{[dt]}$ is the fraction of the driving pattern (%). $K_{[dt]}$ is the correction factor of each driving pattern determined by the model (unitless). Evaporative emissions are also calculated with Eq. (1). $EF_{[t]}$ will be evaporative emission factor of each vehicle technology as the evaporative emissions are calculated.

2.1.2 Road traffic data survey

VKTs and their weights on 3 road types (including highway, arterial road, and residential road) were surveyed from transportation for the year of 2012. VKTs on each road type were further separated into 7 vehicle types by the use of video camera surveys. The distributions of each vehicle type were surveyed on various road types with video cameras from March to May. About 4000 valid hours were obtained on 15 roads covering 3 road types. Survey days included weekdays and weekends and each day covered 24 h. The results show that light-duty vehicles (including light-duty cars, light-duty trucks, and taxis) are the major vehicle types on the road, accounting for 56% of the total flows. Heavy-duty vehicles (including heavy-duty bus, heavy-duty truck, and city bus) comprise 19% of the whole VKTs in Shanghai. GPS data were used to determine the driving patterns of various vehicle types. The driving patterns were determined by the average speeds and VSP (Vehicle Specific Power) distributions. We installed GPS units on light-duty cars, taxis, buses, and heavy-duty trucks to record the driving speeds and altitudes second by second. About 150 hours of valid GPS data were collected in this study. The data covered 2831 km of roads and were composed of 3 road types and 4 vehicle types. VSP of each vehicle and road type can be calculated with Eq. (2) introduced by Jimenez (1999).

$$VSP\left(kW \cdot t^{-1}\right) = v \times \left[1.1a + 9.81 \times \left(a \cdot \tan\left(\sin\left(grade\right)\right)\right) + 0.132\right] + 0.000302 \times v^3 \quad (2)$$

Where, v is vehicle speed ($m \cdot s^{-1}$). a is vehicle acceleration ($m \cdot s^{-2}$). $grade$ is vertical rise/slope length. Table 1 shows the daily VKT and average speeds of various vehicle

and road types in 2012.

2.1.3 Fleet composition data survey

Fleet composition data were used to separate the VKT of each vehicle type (as shown in Table 1) into the fractions of specific technologies, such as fuel type, engine size, and emission standard. The data were determined by the ratios of the populations of specific technologies in the vehicle information database from the Vehicle Management Department of Public Security Bureau of Shanghai. We call this "static" fleet. Light-duty cars and taxis were mainly composed of gasoline vehicles, which occupied 98% and 97%, respectively. Diesel vehicles dominated in light-duty truck, heavy-duty bus, heavy-duty truck, and city bus, comprising 56%, 91%, 89%, and 98%, respectively. Euro 2 vehicles were the majority of light-duty cars and light-duty trucks, accounting for 51% and 68%, respectively. Heavy-duty buses and trucks were mainly composed of Euro 2 and Euro 3 diesel vehicles, which comprised 40% and 45% of each vehicle type. However, the fraction of each specific technology should be changed with its occurrence frequency in the real-world. Generally, older vehicles show less occurrence frequency than newer vehicles, which means the annual mileage of older vehicle should be less than the newer one. For this reason, we considered to adjust the fleet compositions according to their real-world annual average mileages. About 30,000 vehicles were surveyed at 4 inspection stations in this study. Vehicle age and odometer reading were recorded for each vehicle. The survey data showed that the annual average mileages of light-duty truck, heavy-duty bus, and heavy-duty truck tended to decrease with the increase of their vehicle ages. The "adjusted" fleet compositions were determined by the multiplication of vehicle populations and their surveyed annual mileages. Fig. 1 shows the static and adjusted fraction by each vehicle type in Shanghai. It is indicated that the adjusted fractions of the older vehicles with pre-Euro and Euro 1 emission standard for light-duty truck, heavy-duty bus, heavy-duty truck, and city bus were much lower than those of the static ones. Correspondingly, the adjusted fractions of the newer vehicles with Euro 3 emission

standard increased a lot compare with the static ones.

2.1.4 Vehicle emission factors

The emission factors of each vehicle technology were modeled with the IVE model. However, most of the default emission factors in the model are based on the measurements in the US. To localize the emission factors in this study, we collected the published emission factors based on the real-world measurements in the previous studies to adjust the modeled emission factors. The measurements were all conducted with Portable Emission Measurement Systems (PEMS) under designed driving routes in the cities of China. The cities included Shanghai, Beijing, Guangzhou, Xi'an, Shenzhen, Jinan, and Yichang (Chen et al., 2007; Huo et al., 2012a; Huo et al., 2012b; Wu et al., 2012; Huang et al., 2013). Fig. 2 shows the comparisons of the adjusted emission factors with the measured ones. The evaporative emission factors were not adjusted due to the lack of measurement data. Default factors in the model were used to calculate evaporative emissions in this study. It is indicated that the adjusted emission factors of each vehicle type generally fit well with the measured results. The emission factors are reliable to be used to establish the emission inventory.

2.2 VOC species measurements and SOA yield estimation

2.2.1 VOC sampling

The exhaust from 4 light-duty gasoline vehicles (LDGVs), 5 taxis, 5 heavy-duty diesel trucks (HDDTs), 2 city buses (buses), and 5 motorcycles (MTs) were measured in June 2010. LDGVs, taxis, and MTs were fueled by gasoline. HDDTs and buses were fueled by diesel. The emission standards of the tested vehicles covered Euro 1 to Euro 3 and their model years covered 2001 to 2009. All MTs were 4-stroke with 125 cc displacement and without catalytic converter or any other pollution control device. All gasoline vehicles were equipped with catalytic converters. Diesel vehicles didn't install any aftertreatment device like DPF (Diesel Particle Filter). Table 2 lists the detailed information of the tested vehicles. Commercially available fuels were used in the test. The fuel quality met the requirements of the local standard in Shanghai. The

sulfur contents of both gasoline and diesel fuel were below 50 ppm.

All the automobiles were measured on chassis dynamometers. LDGVs and taxis were measured utilizing a vehicle mass analysis system (VMAS), which was widely used in in-use vehicle inspection stations in China. VOC sample was collected from a 1-bag test of the Economic Commission of Europe (ECE) urban cycle. The highest speed reaches 50 $km \cdot h^{-1}$ and the average speed is about 18.8 $km \cdot h^{-1}$. HDDTs and buses were measured on a loaded mode test cycle. The tested vehicles were operated on idling and a test cycle which simulates high engine loads under 100%, 90%, and 80% of their maximum powers. The highest speed reaches 70 $km \cdot h^{-1}$. MT exhausts were sampled while operating on the road. A GPS unit was installed on the tested motorcycles to record the speeds second by second. The highest speed reached 50 $km \cdot h^{-1}$ and the average speed was about 20 $km \cdot h^{-1}$. Vehicle exhaust was sampled into a Summa canister (Entech Inst., USA) during the whole driving cycle. We also collected the samples of gasoline vapor at 4 gas stations in Shanghai to analyze the VOC species of non-tailpipe gasoline.

2.2.2 VOC analysis

Concentration of C2-C12 VOCs in samples were determined by a GC-MS system (Agilent 7890A/5975C) with standard gases prepared by Spectra Gas. The samples collected in the Summa canister were pre-concentrated to an acceptable level for the analytical devices using a 7100A pre-concentrator (Entech Inst., USA) with an Entech 7016CA automatic sample injector. A 50 mL sample was extracted by the pre-concentrator into a 1/4 inch liquid nitrogen cold trap to remove water and CO_2, and then separated by GC and detected by MS. The carrier gas was helium.

2.2.3 SOA yield estimation

To investigate the SOA formation potentials of VOC emissions in vehicle exhausts and gas evaporation, we calculated the SOA yields of the exhausts from gasoline, diesel, and motorcycle vehicles and evaporative emissions with the following equation.

$$Y_j = \frac{\sum \left(C_{i,j} \times Y_i \right)}{\sum VOC_j} \quad (3)$$

Where, Y_j is the SOA yield of source j (unitless). $C_{i,j}$ is the weight percent (by carbon) of species i which can be identified by measurements or references from source j (wtC%). VOC_j is the weight percent (by carbon) of total identified SOA precursors and unidentified species. Identified non-SOA precursors were excluded from total VOC emissions. The weight percentages of identified species were determined by the measurements above. The unidentified species accounted for about 25%, 60%, and 50% in gasoline, diesel, and motorcycle exhausts, repectively. Considering IVOCs which had high SOA formation potentials were not measured in this study, we estimated the amounts of IVOCs including alkanes and aromatics larger than C12 and polycyclic aromatics based on Gentner et al. (2012) and varied them by one order of magnitude. Y_i is the yield of species i under high-NOx condition considering the study was focusing on urban area with high NOx concentration (unitless). The yield for each SOA precursor was referenced from Gentner et al. (2012), which listed the yields of known and estimated compounds using a combination of measured SOA yields derived from laboratory-chamber experiments and approximate SOA yields based on box modeling. However, considering the average organic loading in Shanghai (15.5μg·m^{-3}) was relatively higher than that in the reference (10μg·m^{-3}), we recalculated the SOA yields of the compounds using a semi-empirical model based on absorptive gas-particle partitioning of two semi-volatile products introduced by Odum et al. (1997). The SOA yields of straight alkanes increased by an average of 16% in the range of 12-17 carbon atoms, C6-8 aromatics increased by ~19%, and naphthalene increased by ~12%. The yields of the compounds in similar chemical class were corrected based on the increments above.

247 2.3 Air pollution observation and vehicular OA contribution determination

248 2.3.1 Air pollution observation

249 To estimate the vehicular OA production in the atmosphere, we calculated the
250 SOA formation potentials from vehicular VOC emissions based on observation data
251 with a photochemical- age-based parameterization method. The observation data were
252 obtained from a monitoring site on the roof of a 5-floor building (15 m high above the
253 ground) at Shanghai Academy of Environmental Science (31.17ºN, 121.43ºE), which
254 was located southwest of urban area of Shanghai. The site was mostly surrounded by
255 commercial properties and residential dwellings. Vehicle exhaust was a major source
256 of pollutants near this site. Fig. S1 shows the location of monitoring site in this study.
257 Carbon monoxide was continuously measured by an ECOTECH EC9820 CO analyzer.
258 $PM_{2.5}$ concentration was measured by a Thermo Fisher commercial instrument β-ray
259 particulate monitor. Organic carbon (OC) and elemental carbon (EC) were measured
260 by a carbon analyzer (model RT-4, Sunset Laboratory Inc.). Water soluble ions were
261 measured by a commercial instrument for online monitoring of aerosols and gases
262 (MARGA, model ADI 2080, Applikon Analytical B.V.). Individual VOC species were
263 continuously measured every 30 minutes by two on-line gas chromatographs with
264 flame ionization detector (GC-FID) systems (Chromato-sud airmoVOC C2–C6
265 #5250308 and airmoVOC C6–C12 #2260308, France). Fig. S2 shows the time series
266 data of meteorological parameters and concentrations of major air pollutants observed
267 in urban Shanghai in summer (August in 2013) and winter (January in 2013). We
268 didn't measure the OA concentration due to the lack of observation equipment. The
269 OA concentrations were determined by OC concentrations multiplying the OM/OC
270 ratio. Turpin et al. (2001) suggested a ratio around 1.2-1.6 from fresh emission to aged
271 air mass in remote area. Considering our study was mainly focusing on urban area
272 where emissions were not fully aged, we used the ratio of 1.4 to convert OC
273 concentrations.

2.3.2 OA production estimation

The evolution of primary VOC emissions to SOA formation is determined by OH exposure in the atmosphere. The OH exposure can be calculated with Eq. (4) developed by de Gouw et al. (2005, 2008).

$$\Delta t \cdot [OH] = \frac{1}{(k_X - k_E)} \times \left[\ln\left(\frac{[X]}{[E]}\Big|_{t=0} \right) - \ln\left(\frac{[X]}{[E]} \right) \right] \quad (4)$$

Here, Δt is photochemical age (h). $[OH]$ is the average OH radical concentrations (molecules·cm^{-3}). The ratio of m,p-xylene to ethylbenzene (X/E) was considered as a photochemical clock. k_X and k_E are the OH rate constants of m,p-xylene (18.9×10^{-12} cm^3·molecule^{-1}·s^{-1}) and ethylbenzene (7.0×10^{-12} cm^3·molecule^{-1}·s^{-1}) (Yuan et al., 2013). $[X]/[E]|_{t=0}$ and $[X]/[E]$ are initial emission ratio and the ratio after photochemical reaction of m,p-xylene to ethylbenzene. The concentrations of m,p-xylene and ethylbenzene showed good correlations during the observation (Fig. S3). The different diurnal variations of m,p-xylene and ethylbenzene indicated that they are oxidized at different rates from each other (Fig. S4). Fig. 3 illustrates the diurnal distributions of the ratios of observed m,p-xylene to ethylbenzene in summer and winter of 2013. The initial emission ratios of m,p-xylene to ethylbenzene were determined by the X/E ratio on 97.5 percentiles, which were 2.17 and 1.68 in summer and winter, respectively.

OA production is determined by the loss terms and formation rates of OA concentration after POA emissions exhaust into the atmosphere. de Gouw et al. (2008) introduced a method to explain the OA evolution during photochemical aging of urban plumes as shown by Eq. (5).

$$\begin{aligned} \frac{\Delta OA}{\Delta CO} &= \frac{\Delta POA}{\Delta CO} + \frac{\Delta SOA}{\Delta CO} \\ &= ER_{POA} \times \exp(-L_{OA} \cdot \Delta t) + ER_{VOC_j} \times Y_j \times \frac{P_{OA}}{L_{OA} - P_{OA}} \times \left[\exp(-P_{OA} \cdot \Delta t) - \exp(-L_{OA} \cdot \Delta t) \right] \end{aligned} \quad (5)$$

Here, $\Delta OA/\Delta CO$ is the ratio of OA formation versus CO emission after photochemical reaction (μg·m^{-3}·ppmv^{-1}). ER_{POA} is the primary emission ratio of OA to CO emission (μg·m^{-3}·ppmv^{-1}). ER_{VOCj} is the primary emission ratios of VOC (including SOA

precursors and unidentified species) from source *j* to CO emission in the unit of $ppbv^{-1} \cdot ppmv^{-1}$. Y_j is the SOA yield of source *j*, which is determined by Eq. (3). L_{OA} and P_{OA} are the loss and formation rate of organic aerosol, respectively. We used the empirical parameters derived by de Gouw et al. (2008), which were 0.00677 h^{-1} and 0.0384 h^{-1}, respectively. Δt is the photochemical age calculated by equation (4). Because there is no OH measurement in Shanghai, we reference the 24-h average OH concentration (3×10^6 molecules$\cdot cm^{-3}$) from de Gouw et al. (2008).

2.3.3 Determination of vehicular OA contribution

The observed ΔOA/ΔCO in the atmosphere represents the ratio of total POA emissions and their SOA formation to total CO emissions from all sources, which can be explained by Eq. (6) as follows.

$$\left(\frac{\Delta OA}{\Delta CO}\right)_{obs} = \frac{POA_{total} + SOA_{total}}{CO_{total}} = \frac{\left(POA_{veh} + SOA_{veh}\right)}{CO_{total}} + \frac{\left(POA_{oth} + SOA_{oth}\right)}{CO_{total}} = \frac{OA_{veh}}{CO_{total}} + \frac{OA_{oth}}{CO_{total}} \quad (6)$$

The contribution of vehicular OA to total OA production in the atmosphere can be determined by the ratio of OA_{veh}/CO_{total} to $(\Delta OA/\Delta CO)_{obs}$. Here, $(\Delta OA/\Delta CO)_{obs}$ is the ratio of observed ΔOA (Obs, $OA\text{-}OA_{background}$) to observed ΔCO (Obs, $CO\text{-}CO_{background}$) in the unit of $\mu g \cdot m^{-3} \cdot ppmv^{-1}$. OA_{veh}/CO_{total} is the ratio of vehicular POA emission and SOA formation to total CO emissions, which can be calculated by Eq. (5). ER_{POA} and ER_{VOCj} in Eq. (5) represented for the ratios of vehicular POA and VOC emissions to total CO emissions from vehicles and other sources. The total amount of CO emission was 1.2×10^6 tons according to the annually updated emission inventory in Shanghai for the year of 2012. Iron & steel manufacturing was the major source of CO emission, which accounted for 54% of the total. The sector produced 19.7×10^6 and 18×10^6 tons of pig irons and crude steels, and consumed more than 10×10^6 tons of coal in 2012. Vehicles were the second largest source, accounting for 27.8% of the total. However, considering the observation site was located in the urban area and most of the industrial CO emission sources were located at the surrounding areas (about 30-50 km from city center), it would be more reasonable to simulate the contribution of CO concentration from vehicle exhausts and other sources to the

receptor by using numerical model. Here we used CMAQ model and brute force method to simulate the CO concentrations during January and August in 2013 under two scenarios of with or without vehicular CO emission. The meteorological data was from the results of the Weather Research and Forecasting Model (WRF). Detailed information is shown in the supplement materials. The results showed that vehicles dominated CO emission in urban Shanghai, accounting for 66% and 70% of total CO concentrations in summer and winter, respectively. On this account, the vehicular fraction of total CO emissions used in this study was determined to 68%.

3. Results and discussion

3.1 Vehicle emission inventory

The emissions of CO, NOx, VOCs, EVA (gas evaporation), EC, and POA (OC*1.2) from vehicles were 343.9, 110.9, 39.4, 8.9, 4.0, and 4.3 k tons in Shanghai for the year of 2012 (See Table 3). Gasoline vehicles (including LDGV, Taxi, HDGV, and Motorcycle) were the major sources of CO, VOCs, and EVA emissions, accounting for 91%, 69%, and 100%, respectively. Diesel vehicles (including LDDV, HDDV, and Bus) were the major source of NOx, EC, and POA emissions, comprising 82%, 99%, and 96%, respectively. CO and VOC (including EVA) emissions decreased by 40% and 38% compared with the results for the year of 2004 from Wang et al. (2008). NOx emission increased by 21%. PM emission were low estimated in that article since the PM emission factors were much lower than real-world measurement data as shown in Fig. 2. Gasoline vehicle emissions have been well controlled even though their VKTs were nearly doubled in the past few years. In comparison, the control effect of diesel vehicle emission was relatively poor. It is clear that diesel exhausts dominate the primary PM (including EC and OA) emissions in Shanghai. However, since VOC emissions are mainly from gasoline vehicles, we will further discuss the contributions of gasoline and diesel exhausts to SOA.

354 3.2 VOC species of vehicle emissions and gas evaporation

355 Fig. 4 compares the VOC compositions of the exhausts from different vehicle
356 types and gas evaporation in this study to the results from other countries or regions.
357 Since the VOC species measured in different studies are not the same, we normalized
358 the concentrations of the common species including C2-C12 alkanes, alkenes, alkynes,
359 and single-ring aromatics in each study as 100%. Other compounds and unidentified
360 VOCs were excluded in the comparison. The weighted percentages of individual VOC
361 for the exhausts from different vehicle types and gas evaporation were listed in Table
362 S1.

363 The exhausts from gasoline vehicles (including LDGVs and taxis) had similar
364 VOC compositions. Single-ring aromatics were the major species of the exhausts
365 from gasoline vehicles, accounting for 50% of the total VOCs approximately.
366 Straight-chain alkanes, branched alkanes, and cycloalkanes comprised 17.0%, 18.1%,
367 and 6.1% of the total VOCs, respectively. Toluene, m,p-xylene, o-xylene, and
368 ethylbenzene were the main compounds in LDGV and taxi exhausts, accounting for
369 7.54%, 6.71%, 5.20%, and 4.42% of the total VOCs, respectively. Motorcycle emitted
370 more branched alkanes and less single-ring aromatics than LDGVs and taxis.
371 2-methylhexane (23.43%) was the most abundant VOC in motorcycle exhausts,
372 followed by m,p-xylene (9.34%), ethylbenzene (5.53%) and o-xylene (4.37%). It was
373 indicated from Fig. 3 that the proportion of single-ring aromatics in LDGV exhausts
374 were higher and the proportion of alkene were lower in this and previous studies in
375 China (Liu et al., 2008; Wang et al., 2013) than those in Hong Kong (Guo et al., 2011)
376 and US (Schauer et al., 2002; Gentner et al., 2013; May et al., 2014). The differences
377 of aromatic content in gasoline fuel in different regions and countries could be the
378 main reason of the difference in the proportion of aromatic compounds in LDGV
379 exhausts. The limit of aromatic content in current gasoline standard in China was 40
380 vol%, which was much higher than the limits of gasoline standards of the US (22-25
381 vol%) and Europe (35 vol%).

High proportion of straight-chain alkanes were measured in the exhausts from diesel vehicles, which accounted for 34.9% and 35.6% of the total VOCs from HDDT and bus exhausts, respectively. N-dodecane, propene, n-undecane, acetone, and n-decane were major species in diesel exhausts, accounting for 13.65%, 10.85%, 8.69%, 7.00%, and 6.86% of the total VOCs, respectively. The proportions of straight-chain alkanes in diesel exhausts in this study were much higher than those in the previous studies of the US (Schauer et al., 1999; May et al., 2014). Incomplete combustion of diesel fuel caused by poor engine maintenance could be the main reason for the high straight-chain alkane emissions.

High proportion of alkenes was measured in gas evaporation in this study, which accounted for 40% of the total VOCs. Propane, isopentane, isobutene, 1-pentene, and n-butane were major species in gas evaporation emissions, accounting for 15.99%, 11.87%, 9.69%, 8.87%, and 6.51% of the total VOCs, respectively. The proportions of VOC species in gas evaporation in this study was close to the results in the other study of China (Zhang et al., 2013), but different from the studies in the US (Harley et al., 2000) and Korea (Na et al., 2004), which reported less alkenes and more branched alkanes in gas evaporation.

3.3 SOA yields of different vehicle exhausts and gas evaporation

VOC species of vehicle emissions and gas evaporation were classified into 5 categories by their chemical classes, and their distributions of carbon numbers were shown in Fig. 5(a). Previous studies have confirmed that IVOCs, which were not detected in this study, played important roles to SOA production (Jathar et al., 2013; Zhao et al., 2014). For this reason, we introduced the amounts of alkanes and aromatic larger than C12 and polycyclic aromatics in unburned fuels from Gentner et al. (2012) as the inferred S/IVOCs as shown in the light colored bars in Fig. 5(a). The carbon numbers of VOCs in gasoline and motorcycle exhausts mainly concentrated in the intervals between C6 to C9 whether the IVOCs were merged or not. Comparatively, exhausts from diesel vehicles had a wider distribution of carbon number, ranging from

C2 to C25. More than half of the species were S/IVOCs and most of them were alkanes. The carbon numbers of VOCs in gas evaporation were mainly distributed within the range of C3-C7, which were much smaller than those in vehicle exhausts.

Fig. 5(b) shows the SOA mass yields of different chemical class. To compare the differences of the SOA yields with or without S/IVOC species, we set two scenarios as "Y1" and "Y2". Y1 indicates the SOA yields of measured C2-C12 VOCs in this study. Y2 includes the extra SOA yields of inferred S/IVOCs. S/IVOC species had little effect on the SOA yields of gasoline exhausts and evaporative emissions. Aromatics dominated the yields which accounted for almost 100% of the total. However, the SOA yield of diesel exhaust was significantly affected by S/IVOCs. The yield increased from 0.010 to 0.191 when the inferred S/IVOCs were considered. In Y2 scenario, Aromatics were still the largest contributors (34.9%) to but not dominating the yield. Next were branched alkanes, polycyclic aromatics, and straight-chain alkanes, which accounted for 24.8%, 17.1%, and 12.7%.

The SOA yield of gasoline exhaust was larger than the yield of liquid gasoline reported by Gentner et al. (2012). We found the aromatic contents in gasoline exhausts of this study which dominated the SOA yield were much higher than those in the reference. This may be due to the loose limit of aromatics for the gasoline fuel in China. However, the estimated yield of gasoline exhaust was much lower than the effective yields (3-30%) of LEV-1 (tier 1 of low emission vehicle standard in California, US) gasoline vehicles (similar to Euro 1-3 LDGVs tested in this study) investigated using a smog-chamber experiment by Gordon et al. (2014a). The reason for the underestimate was still unclear. In contrast, the estimated SOA yield of diesel exhaust which combined the inferred S/IVOCs (Y2) was higher than the average effective yields (9±6%) for HDDVs without DPF based on smog-chamber experiments by Gordon et al. (2014b). Since there were few experiments on motorcycle exhaust, we compared the SOA yield of motorcycle exhaust with the experiment results from the exhausts of 2- and 4-stroke gasoline off-road engines

(Gordon et al., 2013). Neither motorcycles nor off-road engines had catalytic converter. The estimated yield was close to the experiment results of off-road engine exhausts (2-4%).

3.4 Primary emission ratio and SOA formation potential based on observation

Fig. 6 is a scatterplot of OA versus CO concentrations measured in urban Shanghai in the summer and the winter of 2013. The observation data were color-coded by OH exposure ($\Delta t \cdot [OH]$) determined by equation (4). It was indicated from the figure that the ratios of OA to CO concentrations generally showed growing trends with the increase of OH exposure both in summer and winter. The results were similar to the previous studies in the United States, Japan, and Mexico (Bahreini et al., 2012; de Gouw et al., 2008; Takegawa et al., 2006; DeCarlo et al., 2008). The primary emission ratios of POA to CO were determined by the minimum slopes of the observed OA to CO concentrations, about 12 $\mu g \cdot m^{-3} \cdot ppmv^{-1}$ in both summer and winter (as shown by the dotted grey lines). The maximum slopes of OA to CO were 50 and 35 $\mu g \cdot m^{-3} \cdot ppmv^{-1}$ (as shown by the dotted black lines) in summer and winter, respectively. The SOA formation ratio in summer was much higher than in winter. The inventory-based vehicular POA emission to total CO emission was 10.6 $\mu g \cdot m^{-3} \cdot ppmv^{-1}$ in the urban area of Shanghai (shown by the dotted yellow lines), close to the primary emission ratio observed in the atmosphere, which indicated that vehicles dominated the POA emissions in urban Shanghai. The dotted pink and orange lines in Fig. 6 represent the maximum OA production ratios (assuming SOA precursors were 100% reacted) calculated with the SOA yields in Y1 (only detected VOCs in this study) and Y2 scenarios (detected VOCs plus the inferred S/IVOCs). The maximum OA production ratios were 13.8 and 18.7 $\mu g \cdot m^{-3} \cdot ppmv^{-1}$, respectively. It was indicated that S/IVOCs played much more important roles to SOA productions of vehicle exhaust. However, the max. OA production ratio for Y2 scenario was still considerable underestimated compared with the observation data, which implied that

466 the SOA yields derived by known and estimated species were still far from explaining
467 the actual SOA formation rate in the atmosphere. For this reason, we introduced the
468 measured SOA yield of gasoline exhaust (~0.190) from Gordon et al. (2014a) to
469 substitute the yield for gasoline vehicles (0.039) in Y2 scenario and defined the new
470 group as Y3 scenario. The maximum OA production ratio (shown by the dotted red
471 lines) increased to 27.6 $\mu g \cdot m^{-3} \cdot ppmv^{-1}$, but still failed to reach the max. observed
472 ΔOA/ΔCO. There must be other emission sources of SOA precursors in the
473 atmosphere of Shanghai. Previous studies have revealed that VOC emissions from
474 solvent usage, chemical and petrochemical industrial, and coal burning, etc.
475 comprised more than 70% of the observed VOCs in the atmosphere of urban Shanghai
476 (Cai et al., 2010; Wang et al., 2013). The SOA productions of VOC emissions from
477 these sources cannot be ignored.

478 3.5 Estimation of vehicular OA contribution in the urban atmosphere

479 Fig. 7 shows the diurnal variations of average observed ΔOA/ΔCO and OH
480 exposure in summer and winter. There was a strong correlation between the observed
481 ΔOA/ΔCO and OH exposure, which indicated the photooxidation dominated the SOA
482 formation in the atmosphere. In the role of photochemical reaction, the observed
483 ΔOA/ΔCO showed rapid growth trend in the afternoon in summer and reached a peak
484 around 13:00~14:00. The average observed ΔOA/ΔCO in urban atmosphere of
485 Shanghai were 33.2 and 21.1 $\mu g \cdot m^{-3} \cdot ppmv^{-1}$ in summer and winter, respectively.

486 To evaluate the contribution of vehicle emission to OA production in urban
487 atmosphere, we estimated the vehicular OA formation ratio to total CO emissions with
488 Eq. (5) in three scenarios. Fig. 7(a) and (b) showed the results of vehicular OA
489 formation ratios to total CO emissions in Y1 scenario. The SOA yields of gasoline,
490 diesel, and motorcycle exhausts and gas evaporation were 0.046, 0.010, 0.024, and
491 0.0009, respectively. Fig. 7(c) and (d) showed the results in Y2 scenario where the
492 inferred S/IVOCs were merged. The SOA yields of gasoline, diesel, and motorcycle
493 exhausts and gas evaporation were 0.047, 0.191, 0.025, and 0.0009, respectively. Fig.

7(e) and (f) showed the results in Y3 scenario. The SOA yield of gasoline exhaust was replaced to 0.190 based on the experiment by Gordon et al. (2014a). The photochemical age (Δt) in each hour was calculated with Eq. (4). Due to the lack of OH measurement in Shanghai, we referenced the 24-h average OH concentration (3×10^6 molecules·cm^{-3}) from de Gouw et al. (2008). The grey and yellow lines were the ratio of vehicular POA and OA production to total CO emissions. The average vehicular OA production ratios to total CO emission in the urban area were 10.6 μg·m^{-3}·ppmv^{-1} and 10.8 μg·m^{-3}·ppmv^{-1} in summer and winter in Y1 scenario, 11.8 μg·m^{-3}·ppmv^{-1} and 11.4 μg·m^{-3}·ppmv^{-1} in Y2 scenario, and 13.3 μg·m^{-3}·ppmv^{-1} and 12.4 μg·m^{-3}·ppmv^{-1} in Y3 scenario. The vehicular OA mass accounted for 34% and 52% of the average observed OA in summer and winter in the urban atmosphere of Shanghai in Y1 scenario. The contributions would increase to 37% and 55% in Y2 scenario, and 41% and 59% in Y3 scenario. It was indicated that vehicle emission was the major source of OA mass in the urban atmosphere of Shanghai. For Y2 scenario where the inferred IVOC species were merged to SOA yield estimation, the vehicular OA production ratios increased about 3%. For Y3 scenario where the SOA yield of gasoline exhausts was enhanced to the smog chamber experiment result (0.190), the vehicular OA production ratios further increased about 4%. Vehicular SOA formation ratios accounted for 4% of the total vehicular OA in Y1 scenario, 9%-13% in Y2 scenario and 16%-23% in Y3 scenario. The SOA formation ratios in both scenarios were lower than expected. There were two possible reasons for the underestimation. One reason was that other emission sources with high SOA formation potentials in addition to vehicles were not considered in this study. The non-fossil VOC emissions from solvent use, chemical and petrochemical industrials, etc. reported by the previous studies could be the rest of contributors (Cai et al., 2010; Wang et al., 2013). Another possible reason was the SOA yields were still underestimated in this study. There were about 30%, 50% and 15% of VOC species still unidentified in gasoline, diesel, and motorcycle exhausts even after we combined the inferred S/IVOC species

reported in Gentner et al. (2012). The SOA formation potentials of the identified VOC species may contribute more SOA than expected.

At present, few SOA observations in the cities of China can be referenced to verify the results in this study. Huang et al. (2014) has reported the fossil OA dominated the OA mass (~40%) in Shanghai based on the observation data in the first quarter of 2013, which was slightly lower than our result. The possible reason for the difference could be the location of observation site (close to urban or suburban). However, the studies both indicated that vehicle emission was the major source of OA mass in large cities of China.

3.6 SOA formation contributions of different vehicle types

Fig. 8(a) and (b) show the changes of OA formation ratios in different fuel and vehicle types in Y1 scenario with the increase of the photochemical age. The OA produced from evaporative emissions were combined in gasoline vehicles and corresponding vehicle types. The inventory-based $\Delta OA/\Delta CO$ show downward trends in Y1 scenario. Diesel exhausts dominated the OA productions, which accounted for 96%, 91% and 84% after 0, 6, and 24 hours of photochemical reaction. HDDV and bus were major sources of OA productions. Fig. 9(c) and (d) show the changes of OA formation ratios in Y2 scenario. The $\Delta OA/\Delta CO$ show upward trends in Y2 scenario. The contributions of diesel exhausts in this scenario increased to 92% and 87% after 6 and 24 hours of photochemical reaction. Fig. 9(e) and (f) show the changes of OA formation ratios in Y3 scenario. The contribution of gasoline vehicles in this scenario increased a lot. Although gasoline vehicles only accounted for 4% of POA emission, their contributions to vehicular OA formation increased to 18% and 34% after 6 and 24 hours of photochemical reaction, respectively. LDGV would be the second large contributor after HDDV. It can be indicated that diesel vehicles were the largest contributors to vehicle derived OA in both scenarios although they only accounted for less than 20% of VKTs in Shanghai. Control of the POA emissions and SOA precursors from diesel vehicles are equally important. Gasoline vehicle could be

another important contributor to vehicular OA formation. However, there still exist some debates on the SOA yield of gasoline exhaust. It will be meaningful to find out their actual SOA yield and key precursors for urban OA pollution control.

4. Conclusions

To evaluate the OA contribution of vehicle emissions in the urban atmosphere of Shanghai, we developed a vehicular emission inventory and estimated the SOA yields of gasoline, diesel, and motorcycle exhausts and gas evaporation based on measured C2-C12 VOC species and inferred S/IVOC species based on Gentner et al. (2012). Higher contents of aromatic were measured in this study and other studies in China compared with the results from the US and European. Loose limit to aromatic contents in the standard of gasoline fuel in China should be responsible for the high aromatic contents, which resulted in larger SOA yield of gasoline exhaust than the results reported by Gentner et al. (2012) based on the same method. However, the estimated yield was still much lower than the results from smog-chamber experiments (Gordon et al., 2014a), which implied the unidentified species were considerable to SOA formation.

Vehicles dominated the POA emissions and OA productions in the urban atmosphere of Shanghai. Their contributions to OA productions were about 40% and 60% in summer and winter, respectively. The rest of the contributors could be the non-fossil VOC emissions from solvent use, chemical and petrochemical industrials, etc. and the underestimated SOA productions from unidentified VOC or IVOC species in the exhausts. At present, vehicles are experiencing rapid growth trends in the cities of China. Primary emissions and secondary formation of OA derived from vehicles will lead to further deterioration of fine particle pollution in the urban area. Reduction of primary PM emissions and SOA precursors from vehicle exhausts will be helpful to improve the air quality in the cities of China. The results also indicate diesel exhausts dominate the POA emissions in the urban area. Therefore, strengthening the primary PM emission control of diesel vehicles, especially for the

older diesel vehicles with loose emission standards as shown by Fig. 2, plays an important role in OA pollution prevention. Now China is conducting the large-scale elimination of "yellow-labeled" diesel vehicles whose emission standards were lower than Euro 3. It can be expected to effectively reduce the OA pollution caused by diesel vehicles. On the other hand, gasoline exhausts have high potential impacts on SOA formation in the urban area. Tightening the limit of aromatic contents in gasoline fuel will be meaningful to reduce the SOA contributions of gasoline vehicles.

There are still some uncertainties need to be improved in the future. First is the SOA mass yield. More experiments on SOA yields of vehicle exhausts in China will be helpful to the SOA formation potentials of different vehicle types. Especially for gasoline exhausts, the estimated SOA yield was much lower than the experiment results in the US. Vehicular OA contributions will increase about 4%-5% if we replace the estimated SOA yield of gasoline exhaust to the experiment result. It will be meaningful to find out their actual SOA yield and key precursors for urban OA pollution control. Emission inventory is another important source of uncertainty in this study. To reduce the uncertainty of vehicular emission inventory, we localized the vehicle mileage and emission factor data based on the traffic surveys in Shanghai and real-world measurements in some cities of China. However, the CO emission inventories of other sources shown in Fig. S5 still have large uncertainties according to the previous study (Huang et al., 2011). More accurate emission inventory will be helpful to reduce the uncertainty of vehicular OA contribution in this study. However, it can be concluded that vehicle emissions are the most important contributors to OA pollution in the cities of China. Another implication is the potential roles of IVOCs in vehicle exhausts are very important on the SOA formation in the urban area. Therefore, further studies need to pay more attentions to determine the contributions of IVOC emissions to OA pollution in China.

Acknowledgement

This study was supported by the National Key Technology R&D Program via

606 grant No. 2014BAC22B03, Chinese Academy of Sciences Strategic Priority Research
607 Program via grant No. XDB05020302, the Science and Technology Commission of
608 Shanghai Municipality Fund Project via grant No. 14DZ1202905, and the Shanghai
609 Natural Science Foundation via grant No. 15ZR1434700.

610 **References**

611 Bahreini, R., Middlebrook, A. M., de Gouw, J. A., Warneke, C., Trainer, M., Brock, C. A.,
612 Stark, H., Brown, S. S., Dube, W. P., Gilman, J. B., Hall, K., Holloway, J. S., Kuster, W.
613 C., Perring, A. E., Prévôt, A. S. H., Schwarz, J. P., Spackman, J. R., Szidat, S., Wagner, N.
614 L., Weber, R. J., Zotter, P., and Parrish, D. D.: Gasoline emissions dominate over diesel
615 in formation of secondary organic aerosol mass, Geophys. Res. Lett., 39, L06805,
616 doi:10.1029/2011GL050718, 2012.

617 Borbon, A., Gilman, J. B., Kuster, W. C., Grand, N., Chevaillier, S., Colomb, A., Dolgorouky,
618 C., Gros, V., Lopez, M., Sarda-Esteve, R., Holloway, J., Stutz, J., Petetin, H., McKeen, S.,
619 Beekmann, M., Warneke, C., Parrish, D. D., and de Gouw, J. A.: Emission ratios of
620 anthropogenic volatile organic compounds in northern mid-latitude megacities:
621 Observations versus emission inventories in Los Angeles and Paris, J. Geophys.
622 Res.-Atmos., 118, 2041–2057, doi:10.1002/jgrd.50059, 2013

623 Cai, C. J., Geng, F. H., Tie, X. X., Yu, Q., An, J. L.: Characteristics and source apportionment
624 of VOCs measured in Shanghai, China, Atmospheric Environment, 44, 5005–5014,
625 2010.

626 Cao, J. J., Zhu, C. S., Tie, X. X., Geng, F. H., Xu, H. M., Ho, S. S. H., Wang, G. H., Han, Y.
627 M., Ho., K.F.: Characteristics and sources of carbonaceous aerosols from Shanghai,
628 China. Atmos. Chem. Phys., 13, 803–817, 2013.

629 Chan, A. W. H., Kautzman, K. E., Chhabra, P. S., Surratt, J. D., Chan, M. N., Crounse, J. D.,
630 Kürten, A., Wennberg, P. O., Flagan, R. C., and Seinfeld, J. H.: Secondary organic
631 aerosol formation from photooxidation of naphthalene and alkylnaphthalenes:
632 implications for oxidation of intermediate volatility organic compounds (IVOCs), Atmos.
633 Chem. Phys., 9, 3049–3060, doi:10.5194/acp-9-3049-2009, 2009.

634 Chen, C. H., Huang, C., Jing, Q. G., Wang, H. K., Pan, H. S., Li, L., Zhao, J., Dai, Y., Huang,
635 H. Y., Schipper, L., Streets, D. G.: On-road emission characteristics of heavy-duty diesel
636 vehicles in Shanghai, Atmospheric Environment, 41, 5334-5344, 2007.
637 Chirico, R., DeCarlo, P. F., Heringa, M. F., Tritscher, T., Richter, R., Prévôt, A. S. H.,
638 Dommen, J., Weingartner, E., Wehrle, G., Gysel, M., Laborde, M., and Baltensperger, U.:
639 Impact of aftertreatment devices on primary emissions and secondary organic aerosol
640 formation potential from in-use diesel vehicles: results from smog chamber experiments,
641 Atmos. Chem. Phys., 10, 11545–11563, doi:10.5194/acp-10-11545-2010, 2010.
642 DeCarlo, P. F., Dunlea, E. J., Kimme, J. R., Aiken, A. C., Sueper, D., Crounse, J., Wennberg, P.
643 O., Emmons, L., Shinozuka, Y., Clarke, A., Zhou, J., Tomlinson, J., Collins, D. R.,
644 Knapp, D., Weinheimer, A. J., Montzka, D. D., Campos, T., Jimenez, J. L.: Fast airborne
645 aerosol size and chemistry measurements above Mexico City and Central Mexico during
646 the MILAGRO campaign, Atmos. Chem. Phys., 8, 4027–4048, 2008.
647 de Gouw, J. A., Middlebrook, A. M., Warneke, C., Goldan, P. D., Kuster, W. C., Roberts, J. M.,
648 Fehsenfeld, F. C., Worsnop, D. R., Canagaratna, M. R., Pszenny, A. A. P., Keene, W. C.,
649 Marchewka, M., Bertman, S. B., and Bates, T. S.: Budget of organic carbon in a polluted
650 atmosphere: Results from the New England Air Quality Study in 2002, J. Geophys.
651 Res.-Atmos., 110, D16305, doi:10.1029/2004jd005623, 2005.
652 de Gouw, J. A., Brock, C. A., Atlas, E. L., Bates, T. S., Fehsenfeld, F. C., Goldan, P. D.,
653 Holloway, J. S., Kuster, W. C., Lerner, B. M., Matthew, B. M., Middlebrook, A. M.,
654 Onasch, T. B., Peltier, R. E., Quinn, P. K., Senff, C. J., Stohl, A., Sullivan, A. P., Trainer,
655 M., Warneke, C., Weber, R. J., and Williams, E. J.: Sources of particulate matter in the
656 northeastern United States in summer: 1. Direct emissions and secondary formation of
657 organic matter in urban plumes, J. Geophys. Res.-Atmos., 113, D08301,
658 doi:08310.01029/02007JD009243, 2008.
659 de Gouw, J. and Jimenez, J. L.: Organic Aerosols in the Earth's Atmosphere, Environ. Sci.
660 Technol., 43, 7614–7618, 2009.
661 Feng, J. L., Chan, C. K., Fang, M., Hu, M., He, L. Y., Tang, X. Y.: Characteristics of organic

matter in $PM_{2.5}$ in Shanghai, Chemosphere, 64, 1393-1400, 2005.

Feng, J. L., Li, M., Zhang, P., Gong, S. Y., Zhong, M., Wu, M. H., Zheng, M., Chen, C. H., Wang, H. L., Lou, S. R.: Investigation of the sources and seasonal variations of secondary organic aerosols in $PM_{2.5}$ in Shanghai with organic tracers, Atmospheric Environment, 79, 614-622, 2013.

Feng, Y. L., Chen, Y. J., Guo, H., Zhi, G. R., Xiong, S. C., Li, J., Sheng, G. Y., Fu, J. M.: Characteristics of organic and elemental carbon in $PM_{2.5}$ samples in Shanghai, China, Atmospheric Research, 92, 434-442, 2009.

Gentner, D. R., Isaacman, G., Worton, D. R., Chan, A. W. H., Dallmann, T. R., Davis, L., Liu, S., Day, D. A., Russell, L. M., Wilson, K. R., Weber, R., Uha, A., Harley, R. A., and Goldstein, A. H.: Elucidating secondary organic aerosol from diesel and gasoline vehicles through detailed characterization of organic carbon emissions, P. Natl. Acad. Sci. USA, 109, 18318–18323, 2012.

Gentner, D. R., Worton, D. R., Isaacman, G., Davis, L. C., Dallmann, T. R., Wood, E. C., Herndon, S. C., Goldstein, A. H., Harley, R. A.: Chemical composition of gas-phase organic carbon emissions from motor vehicles and implications for ozone production, Environ. Sci. Technol., 47, 11837−11848, 2013.

Gordon, T. D., Tkacik, D. S., Presto, A. A., Zhang, M., Jathar, S. H., Nguyen, N. T., Massetti, J., Truong, T., Cicero-Fernandez, P., Maddox, C., Rieger, P., Chattopadhyay, S., Maldonado, H., Maricq, M. M., Robinson, A. L.: Primary gas- and particle-phase emissions and secondary organic aerosol production from gasoline and diesel off-road engines, Environ. Sci. Technol., 47, 14137−14146, 2013.

Gordon, T. D., Presto, A. A., May, A. A., Nguyen, N. T., Lipsky, E. M., Donahue, N. M., Gutierrez, A., Zhang, M., Maddox, C., Rieger, P., Chattopadhyay, S., Maldonado, H., Maricq, M. M., Robinson, A. L.: Secondary organic aerosol formation exceeds primary particulate matter emissions for light-duty gasoline vehicles, Atmos. Chem. Phys., 14, 4661–4678, 2014a.

Gordon, T. D., Presto, A. A., Nguyen, N. T., Robertson, W. H., Na, K., Sahay, K. N., Zhang,

690 M., Maddox, C., Chattopadhyay, S., Maldonado, H., Maricq, M. M., Robinson, A. L.:
691 Secondary organic aerosol production from diesel vehicle exhaust: impact of
692 aftertreatment, fuel chemistry and driving cycle, Atmos. Chem. Phys., 14, 4643–4659,
693 2014b.
694 Grieshop, A. P., Donahue, N. M., and Robinson, A. L.: Laboratory investigation of
695 photochemical oxidation of organic aerosol from wood fires 2: analysis of aerosol mass
696 spectrometer data, Atmos. Chem. Phys., 9, 2227–2240, 2009.
697 Guo, H., Zou, S. C., Tsai, W. Y., Chan, L. Y., Blake, D. R.: Emission characteristics of
698 nonmethane hydrocarbons from private cars and taxis at different driving speeds in Hong
699 Kong, Atmospheric Environment, 45, 2711–2721, 2011.
700 Hallquist, M., Wenger, J. C., Baltensperger, U., Rudich, Y., Simpson, D., Claeys, M.,
701 Dommen, J., Donahue, N. M., George, C., Goldstein, A. H., Hamilton, J. F., Herrmann,
702 H., Hoffmann, T., Iinuma, Y., Jang, M., Jenkin, M. E., Jimenez, J. L., Kiendler-Scharr, A.,
703 Maenhaut, W., McFiggans, G., Mentel, Th. F., Monod, A., Prévôt, A. S. H., Seinfeld, J.
704 H., Surratt, J. D., Szmigielski, R., and Wildt, J.: The formation, properties and impact of
705 secondary organic aerosol: current and emerging issues, Atmos. Chem. Phys., 9,
706 5155–5236, doi:10.5194/acp-9-5155-2009, 2009.
707 Harley, R. A., Coulter-Burke, S. C., Yeung, T. S.: Relating liquid fuel and headspace vapor
708 composition for California reformulated gasoline samples containing ethanol, Environ.
709 Sci. Technol., 34, 4088–4094, 2000.
710 Hayes, P. L., Ortega, A. M., Cubison, M. J., Froyd, K. D., Zhao, Y., Cliff, S. S., Hu, W. W.,
711 Toohey, D. W., Flynn, J. H., Lefer, B. L., Grossberg, N., Alvarez, S., Rappengluck, B.,
712 Taylor, J. W., Allan, J. D., Holloway, J. S., Gilman, J. B., Kuster, W. C., de Gouw, J. A.,
713 Massoli, P., Zhang, X., Liu, J., Weber, R. J., Corrigan, A. L., Russell, L. M., Isaacman, G.,
714 Worton, D. R., Kreisberg, N. M., Goldstein, A. H., Thalman, R., Waxman, E. M.,
715 Volkamer, R., Lin, Y. H., Surratt, J. D., Kleindienst, T. E., Offenberg, J. H., Dusanter, S.,
716 Griffith, S., Stevens, P. S., Brioude, J., Angevine, W. M., Jimenez, J. L.: Organic aerosol
717 composition and sources in Pasadena, California during the 2010 CalNex Campaign, J.

718 Geophys. Res.-Atmos., 118, 9233–9257, doi:10.1002/jgrd.50530, 2013.
719 Hou, B., Zhuang, G. S., Zhang, R., Liu, T. N., Guo, Z. G., Chen, Y.: The implication of
720 carbonaceous aerosol to the formation of haze: Revealed from the characteristics and
721 sources of OC/EC over a mega-city in China, Journal of Hazardous Materials, 190,
722 529–536, 2011.
723 Huang, C., Chen, C. H., Li, L., Cheng, Z., Wang, H. L., Huang, H. Y., Streets, D. G., Wang, Y.
724 J., Zhang, G. F., and Chen, Y. R.: Emission inventory of anthropogenic air pollutants and
725 VOC species in the Yangtze River Delta region, China, Atmos. Chem. Phys., 11,
726 4105–4120, doi:10.5194/acp-11-4105-2011, 2011.
727 Huang, C., Lou, D. M., Hu, Z. Y., Feng, Q., Chen, Y. R., Chen, C. H., Tan, P. Q., Yao, D.: A
728 PEMS study of the emissions of gaseous pollutants and ultrafine particles from gasoline-
729 and diesel-fueled vehicles, Atmospheric Environment, 77, 703–710, 2013.
730 Huang, R. J., Zhang, Y. L., Bozzetti, C., Ho, K. F., Cao, J. J., Han, Y. M., Daellenbach, K. R.,
731 Slowik, J. G., Platt, S. M., Canonaco, F., Zotter, P., Wolf, R., Pieber, S. M., Bruns, E. A.,
732 Crippa, M., Ciarelli, G., Piazzalunga, A., Schwikowski, M., Abbaszade, G.,
733 Schnelle-Kreis, J., Zimmermann, R., An, Z., Szidat, S., Baltensperger, U., El Haddad, I.,
734 Prévôt, A. S. H.: High secondary aerosol contribution to particulate pollution during haze
735 events in China, Nature, 514, 218–222, doi:10.1038/nature13774, 2014.
736 Huang, X. F., He, L. Y., Xue, L., Sun, T. L., Zeng, L. W., Gong, Z. H., Hu, M., Zhu, T.: Highly
737 time-resolved chemical characterization of atmospheric fine particles during 2010
738 Shanghai World Expo, Atmos. Chem. Phys., 12, 4897–4907,
739 doi:10.5194/acp-12-4897-2012, 2012.
740 Huang, X. F., Xue, L., Tian, X. D., Shao, W. W., Sun, T. L., Gong, Z. H., Ju, W. W., Jiang, B.,
741 Hu, M., He, L. Y.: Highly time-resolved carbonaceous aerosol characterization in
742 Yangtze River Delta of China: Composition, mixing state and secondary formation,
743 Atmospheric Environment, 64, 200-207, 2013.
744 Hung, H. F. and Wang, C. S.: Formation of secondary organic aerosols and reactive oxygen
745 species from diluted motorcycle exhaust, J. Chin. Inst. Chem. Eng., 37, 491−499, 2006.

746 Huo, H., Yao, Z. L., Zhang, Y. Z., Shen, X. B., Zhang, Q., Ding, Y., He, K. B.: On-board
747 measurements of emissions from light-duty gasoline vehicles in three mega-cities of
748 China, Atmospheric Environment, 49, 371-377, 2012a.
749 Huo, H., Yao, Z. L., Zhang, Y. Z., Shen, X. B., Zhang, Q., He, K. B.: On-board measurements
750 of emissions from diesel trucks in five cities in China, Atmospheric Environment, 54,
751 159-167, 2012b.
752 Jathar, S. H., Miracolo, M. A., Tkacik, D. S., Donahue, N. M., Adams, P. J., and Robinson, A.
753 L.: Secondary organic aerosol formation from photo-oxidation of unburned fuel:
754 Experimental results and implications for aerosol formation from combustion emissions,
755 Environ. Sci. Technol., 47, 12886−12893, 2013.
756 Jimenez, J. L.: Ph. D thesis of Understanding and quantifying motor vehicle emissions with
757 vehicle specific power and TILDAS remote sensing, Massachusetts: Massachusetts
758 Institute of Technology, 1999.
759 Jimenez, J. L., Canagaratna, M. R., Donahue, N. M., Prévôt, A. S. H., Zhang, Q., et al.:
760 Evolution of organic aerosols in the atmosphere, Science, 326 (5959), 1525−1529, 2009.
761 Kleindienst, T. E., Corse, E.W., Li,W., McIver, C. D., Conver, T. S., Edney, E. O., Driscoll, D.
762 J., Speer, R. E., Weathers, W. S., and Tejada, S. B.: Secondary organic aerosol formation
763 from the irradiation of simulated automobile exhaust, J Air Waste Manage., 52, 259–272,
764 2002.
765 Liu, S., Ahlm, L., Day, D. A., Russell, L. M., Zhao, Y. L., Gentner, D. R., Weber, R. J.,
766 Goldstein, A. H., Jaoui, M., Offenberg, J. H., Kleindienst, T. E., Rubitschun, C., Surratt,
767 J. D., Sheesley, R. J., and Scheller, S.: Secondary organic aerosol formation from fossil
768 fuel sources contribute majority of summertime organic mass at Bakersfield, J. Geophys.
769 Res.-Atmos., 117, D00V26, doi:10.1029/2012JD018170, 2012
770 Liu, Y., Shao, M., Fu, L. L., Lu, S.H., Zeng, L. M., Tang, D. G.: Source profiles of volatile
771 organic compounds (VOCs) measured in China: Part I, Atmospheric Environment, 42,
772 6247–6260, 2008.
773 May, A.A., Nguyen, N.T., Presto, A.A., Gordon, T.D., Lipsky, E.M., Karve, M., Gutierrez, A.,

774 Robertson, W.H., Zhang, M., Brandow, C., Chang, O., Chen, S., Cicero-Fernandez, P.,
775 Dinkins, L., Fuentes, M., Huang, S.M., Ling, R., Long, J., Maddox, C., Massetti, J.,
776 McCauley, E., Miguel, A., Na, K., Ong, R., Pang, Y., Rieger, P., Sax, T., Truong, T., Vo,
777 T., Chattopadhyay, S., Maldonado, H., Maricq, M.M., Robinson, A.L.: Gas- and
778 particle-phase primary emissions from in-use, on-road gasoline and diesel vehicles,
779 Atmospheric Environment, 88, 247–260, 2014.
780 Na, K., Kim, Y. P., Moon, I., Moon, K. C.: Chemical composition of major VOC emission
781 sources in the Seoul atmosphere, Chemosphere, 55, 585–594, 2004.
782 Ng, N. L., Kroll, J. H., Chan, A. W. H., Chhabra, P. S., Flagan, R. C., and Seinfeld, J. H.:
783 Secondary organic aerosol formation from m-xylene, toluene, and benzene, Atmos.
784 Chem. Phys., 7, 3909–3922, doi:10.5194/acp-7-3909-2007, 2007.
785 Nordin, E. Z., Eriksson, A. C., Roldin, P., Nilsson, P. T., Carlsson, J. E., Kajos, M. K., Hellén,
786 H.,Wittbom, C., Rissler, J., Löndahl, J., Swietlicki, E., Svenningsson, B., Bohgard, M.,
787 Kulmala, M., Hallquist, M., and Pagels, J. H.: Secondary organic aerosol formation from
788 idling gasoline passenger vehicle emissions investigated in a smog chamber, Atmos.
789 Chem. Phys., 13, 6101–6116, doi:10.5194/acp-13-6101-2013, 2013.
790 Odum, J. R., Jungkamp, T. P. W., Griffin, R. J., Forstner, H. J. L., Flagan, R. C., and Seinfeld,
791 J. H.: Aromatics, reformulated gasoline, and atmospheric organic aerosol formation,
792 Environ. Sci. Technol., 31, 1890–1897, 1997.
793 Platt S. M., El Haddad, I., Zardini, A. A., Clairotte, M., Astorga, C., Wolf, R., Slowik, J. G.,
794 Temime-Roussel, B., Marchand, N., Ježek, I., Drinovec, L., Močnik, G., Möhler, O.,
795 Richter, R., Barmet, P., Bianchi, F., Baltensperger, U., and Prévôt, A. S. H.: Secondary
796 organic aerosol formation from gasoline vehicle emissions in a new mobile
797 environmental reaction chamber, Atmos. Chem. Phys., 13, 9141–9158,
798 doi:10.5194/acp-13-9141-2013, 2013.
799 Robinson, A. L., Donahue, N. M., Shrivastava, M. K., Weitkamp, E. A., Sage, A. M.,
800 Grieshop, A. P., Lane, T. E., Pierce, J. R., and Pandis, S. N.: Rethinking organic aerosols:
801 Semivolatile emissions and photochemical aging, Science, 315, 1259–1262, 2007.

SCCTPI (Shanghai City Comprehensive Transportation Planning Institute): Shanghai comprehensive transportation annual report, Shanghai, 2012.

Schauer, J. J., Kleeman, M., Cass, G., Simoneit, B. T.: Measurement of emissions from air pollution sources. 2. C1 through C30 organic compounds from medium duty diesel trucks, Environ. Sci. Technol., 33, 1578–1587, 1999.

Schauer, J. J., Kleeman, M., Cass, G., Simoneit, B. T.: Measurement of emissions from air pollution sources. 5. C1-C32 organic compounds from gasoline-powered motor vehicles, Environ. Sci. Technol., 36, 1169–1180, 2002.

Stone, E. A., Zhou, J., Snyder, D. C., Rutter, A. P., Mieritz, M., and Schauer, J. J.: A comparison of summertime secondary organic aerosol source contributions at contrasting urban locations, Environ. Sci. Technol., 43, 3448–3454, 2009.

Takegawa, N., Miyakawa, T., Kondo, Y., Jimenez, J. L., Zhang, Q., Worsnop, D. R., Fukuda, M.: Seasonal and diurnal variations of submicron organic aerosol in Tokyo observed using the Aerodyne aerosol mass spectrometer, J. Geophys. Res.-Atmos., 111, D11206, doi:10.1029/2005JD006515, 2006.

Turpin, B. J. and Lim, H. J.: Species contributions to $PM_{2.5}$ mass concentrations: Revisiting common assumptions for estimating organic mass, Aerosol Science and Technology, 35, 602-610, 2001.

Wang, H. K., Chen, C. H., Huang, C., Fu, L.X.: On-road vehicle emission inventory and its uncertainty analysis for Shanghai, China. Science of the Total Environment, 398, 60–67, 2008.

Wang, H. L., Chen, C. H., Wang, Q., Huang, C., Su, L. Y., Huang, H. Y., Lou, S. R., Zhou, M., Li, L., Qiao, L. P., Wang, Y. H.: Chemical loss of volatile organic compounds and its impact on the source analysis through a two-year continuous measurement, Atmospheric Environment, 80, 488–498, 2013.

Wang, J., Jin, L. M., Gao, J. H., Shi, J. W., Zhao, Y. L., Liu, S. X., Jin, T. S., Bai, Z. P., Wu, C. Y.: Investigation of speciated VOC in gasoline vehicular exhaust under ECE and EUDC test cycles, Science of the Total Environment, 445–446, 110–116, 2013.

Warneke, C., de Gouw, J. A., Goldan, P. D., Kuster, W. C., Williams, E. J., Lerner, B. M., Jakoubek, R., Brown, S. S., Stark, H., Aldener, M., Ravishankara, A. R., Roberts, J. M., Marchewka, M., Bertman, S., Sueper, D. T., McKeen, S. A., Meagher, J. F., and Fehsenfeld, F. C.: Comparison of daytime and nighttime oxidation of biogenic and anthropogenic VOCs along the New England coast in summer during New England Air Quality Study 2002, J. Geophys. Res.-Atmos., 109, D10309, doi:10.1029/2003jd004424, 2004.

Weitkamp, E. A., Sage, A. M., Pierce, J. R., Donahue, N. M., and Robinson, A. L.: Organic aerosol formation from photochemical oxidation of diesel exhaust in a smog chamber, Environ. Sci. Technol., 41, 6969–6975, 2007.

Wu, Y., Zhang, S. J., Li, M. L., Ge, Y. S., Shu, J. W., Zhou, Y., Xu, Y. Y., Hu, J. N., Liu, H., Fu, L. X., He, K. B., Hao, J. M.: The challenge to NOx emission control for heavy-duty diesel vehicles in China, Atmos. Chem. Phys., 12, 9365–9379, 2012.

Ye, B. M., Ji, X. L., Yang, H. Z., Yao, X. H., Chan, C. K., Cadle, S. H., Chan, T., Mulawa, P. A.: Concentration and chemical composition of $PM_{2.5}$ in Shanghai for a 1-year period, Atmospheric Environment, 37, 499–510, 2003.

Yuan, B., Hu, W. W., Shao, M., Wang, M., Chen, W. T., Lu, S. H., Zeng, L. M., and Hu, M.: VOC emissions, evolutions and contributions to SOA formation at a receptor site in eastern China, Atmos. Chem. Phys., 13, 8815–8832, doi:10.5194/acp-13-8815-2013, 2013.

Zhang, Y. L., Wang, X. M., Zhang, Z., Lü, S. J., Shao, M., Lee, S. C., Yu, J. Z.: Species profiles and normalized reactivity of volatile organic compounds from gasoline evaporation in China, Atmospheric Environment, 79, 110–118, 2013.

Zhao, Y. L., Hennigan, C. J., May, A. A., Tkacik, D. S., de Gouw, J. A., Gilman, J. B., Kuster, W. C., Borbon, A., Robinson, A. L.: Intermediate-volatility organic compounds: a large source of secondary organic aerosol, Environ. Sci. Technol., 48, 13743−13750, 2014.

856

857 **Table 1.** Daily VKT and average speeds of various vehicle and road types in Shanghai in 2012.

Road types	Daily vehicle kilometers traveled (million km)								Average speed ($km \cdot h^{-1}$)
	Light-duty car	Light-duty truck	Taxi	Heavy-duty bus	Heavy-duty truck	City bus	Motor-cycle	Total	
Highway	38.3	0.62	3.96	3.10	11.82	0.23	0.00	58.04	57.9
Arterial road	22.6	2.93	6.16	1.12	4.73	1.58	5.29	44.41	36.0
Residential road	18.3	3.11	8.92	0.89	1.90	1.38	4.15	38.64	28.5
Total	79.2	6.66	19.04	5.11	18.45	3.19	9.44	141.09	43.0

858

859

860 **Table 2.** Test vehicle specifications.

ID	Vehicle type	Fuel type	Emission standard	Model year	Odometer reading (km)
LDGV-1	Light-duty car	Gasoline	Euro 1	2002	245306
LDGV-2	Light-duty car	Gasoline	Euro 2	2005	59790
LDGV-3	Light-duty car	Gasoline	Euro 3	2008	87662
LDGV-4	Light-duty car	Gasoline	Euro 3	2008	80856
Taxi-1	Light-duty taxi	Gasoline	Euro 1	2001	270000
Taxi-2	Light-duty taxi	Gasoline	Euro 1	2002	~100000
Taxi-3	Light-duty taxi	Gasoline	Euro 2	2003	99638
Taxi-4	Light-duty taxi	Gasoline	Euro 3	2007	281315
Taxi-5	Light-duty taxi	Gasoline	Euro 3	2008	361180
HDDT-1	Heavy-duty truck	Diesel	Euro 1	2003	331387
HDDT-2	Heavy-duty truck	Diesel	Euro 1	2003	271000
HDDT-3	Heavy-duty truck	Diesel	Euro 2	2004	271125
HDDT-4	Heavy-duty truck	Diesel	Euro 2	2004	204193
HDDT-5	Heavy-duty truck	Diesel	Euro 3	2009	70000
Bus-1	City bus	Diesel	Euro 2	2006	295236
Bus-2	City bus	Diesel	Euro 3	2006	175122
MT-1	Motorcycle	Gasoline	Euro 1	2003	15000
MT-2	Motorcycle	Gasoline	Euro 1	2003	11191
MT-3	Motorcycle	Gasoline	Euro 2	2004	96969
MT-4	Motorcycle	Gasoline	Euro 2	2003	13912
MT-5	Motorcycle	Gasoline	Euro 2	2003	5379

861

862

863

864

865 **Table 3.** Vehicle emission inventory in Shanghai.

Vehicle type	Emission inventory (k ton)					
	CO	NOx	VOCs	EVA	EC	POA (OC*1.2)
in vehicle type						
LDGV	192.03	13.30	15.59	6.15	0.02	0.07
LDDV	1.89	5.72	0.32	0.00	0.17	0.11
Taxi	68.89	3.86	5.56	1.96	0.01	0.03
HDGV	36.79	2.20	2.29	0.29	0.00	0.01
HDDV	24.71	67.56	9.74	0.00	3.16	3.40
Bus	5.53	17.56	2.06	0.00	0.58	0.62
Motorcycle	14.01	0.67	3.85	0.49	0.02	0.06
in fuel type						
Gasoline	311.71	20.04	27.28	8.88	0.05	0.17
Diesel	32.14	90.84	12.12	0.00	3.91	4.13
Total	343.85	110.88	39.40	8.88	3.96	4.30

866

867

868

869

870

871

872

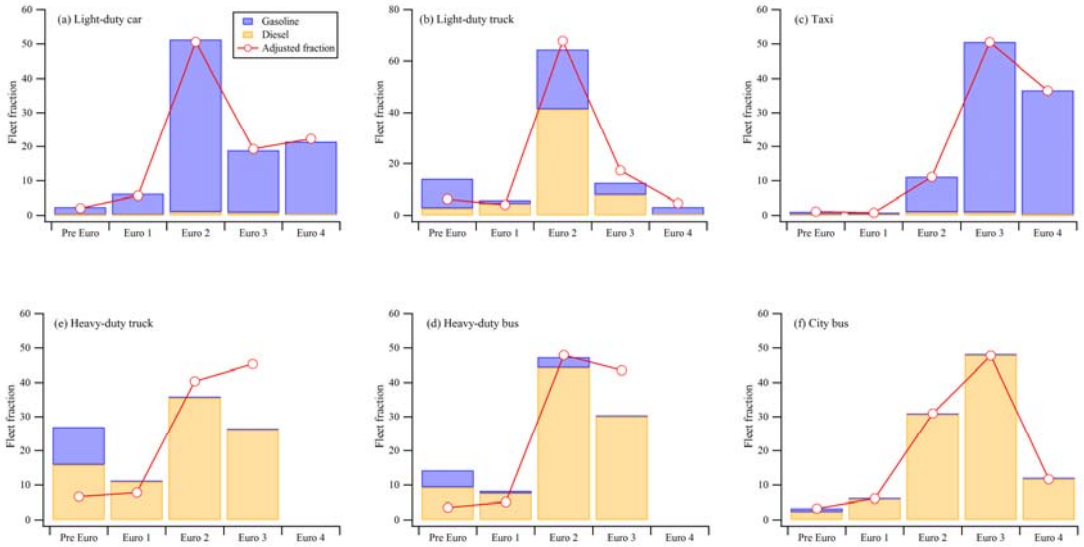

Fig. 1. Static and adjusted fractions of each vehicle type in Shanghai.

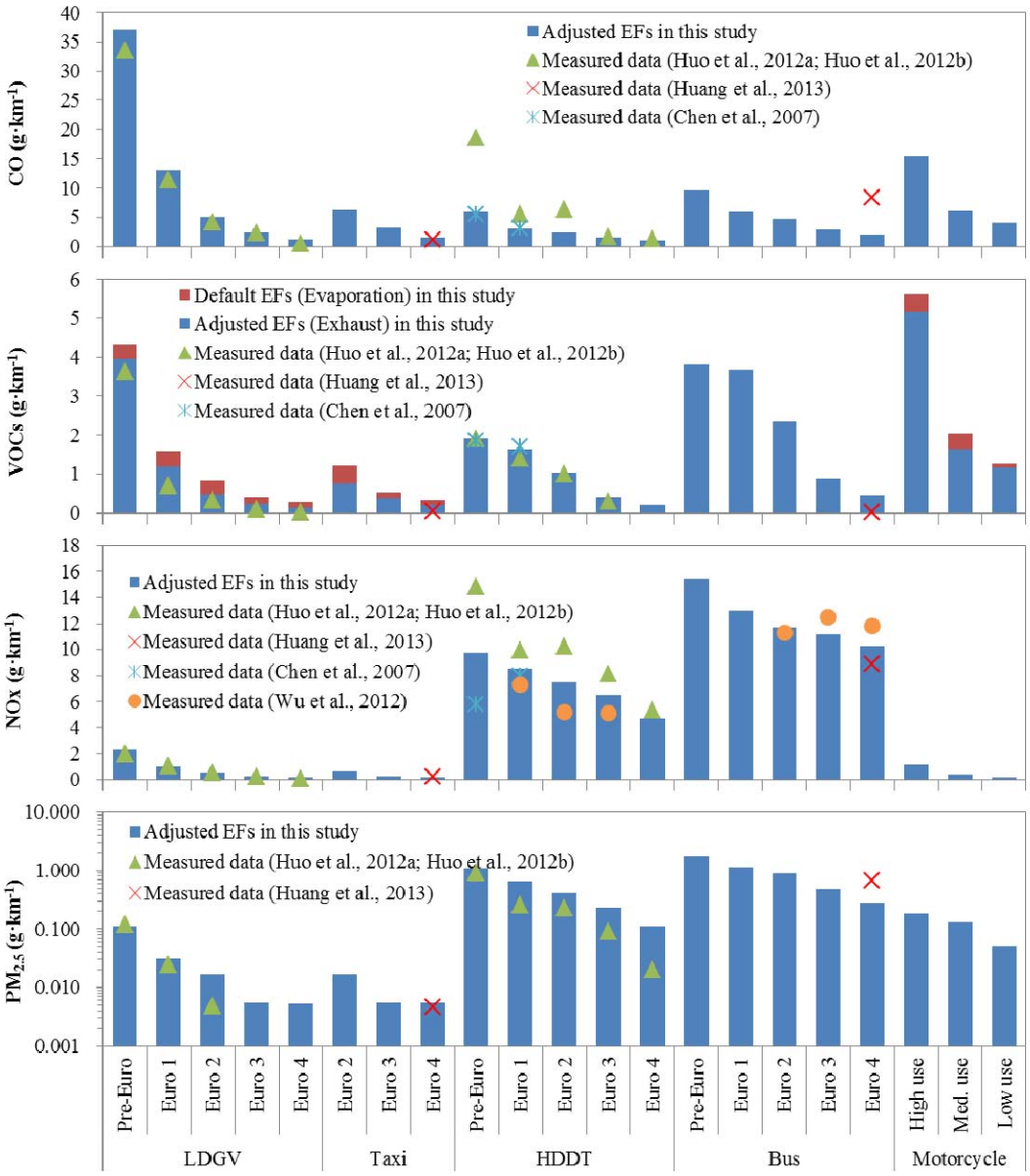

Fig. 2. Adjusted emission factors of various vehicle types (blue bars) and their comparisons with measured emission factors in the previous studies (dots).

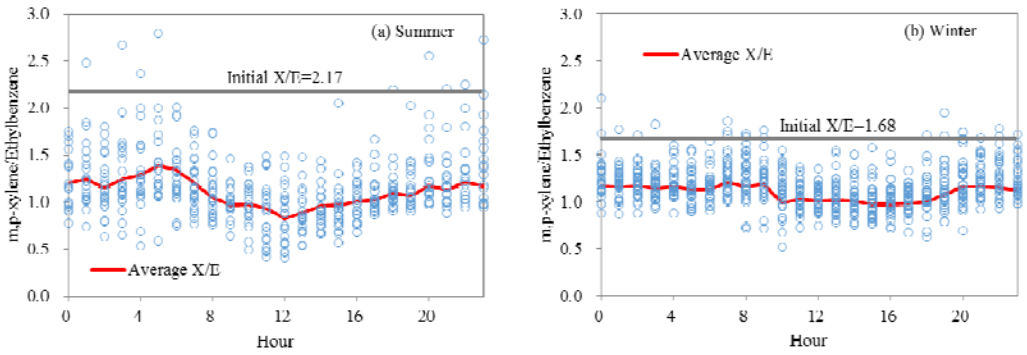

886

887 **Fig. 3.** Diurnal distributions of the ratios of m,p-xylene to ethylbenzene concentrations in summer

888 and winter in the urban atmosphere in 2013.

889

890

891

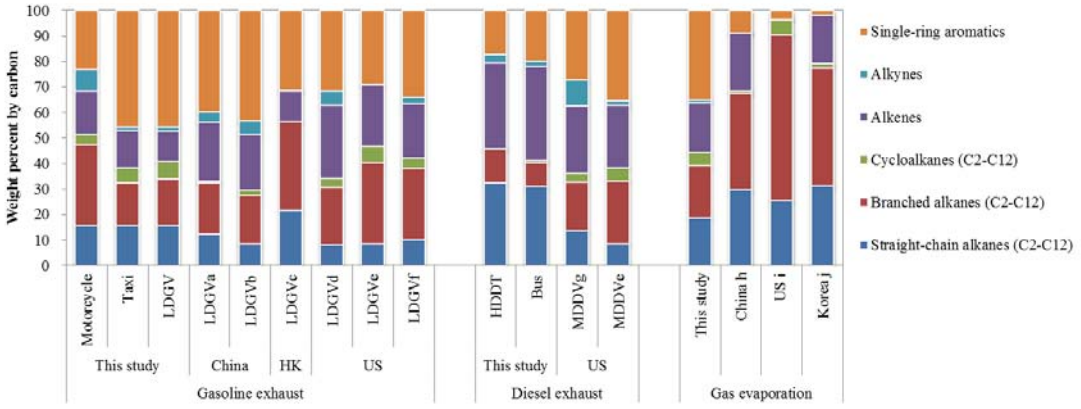

892

893 **Fig. 4.** Comparisons of measured VOC compositions of the exhausts from different vehicle types

894 and gas evaporation to the results in other studies (a. Liu et al., 2008; b. Wang et al., 2013; c. Guo

895 et al., 2011; d. Schauer et al., 2002; e. May et al., 2014; f. Gentner et al., 2013; g. Schauer et al.,

896 1999; h. Zhang et al., 2013; i. Harley et al., 2000; j. Na et al., 2004).

897

898

899

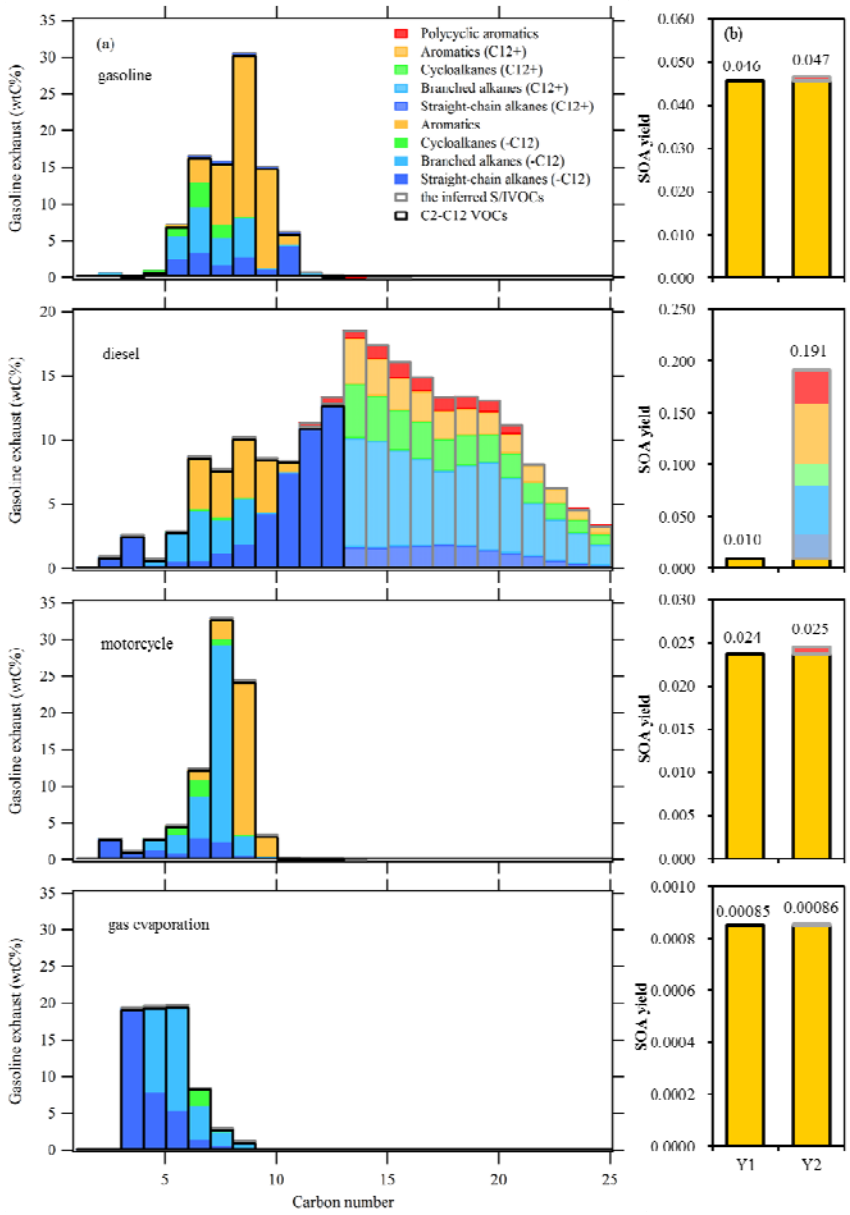

Fig. 5. (a) Distributions of mass by chemical class in carbon number of different vehicle exhausts and evaporative emissions; (b) Calculated SOA yields based on C2-C12 VOCs measured in this study (Y1) and C2-C12 VOCs plus the inferred S/IVOC species (Y2). The inferred S/IVOC species are shown in light colored bars.

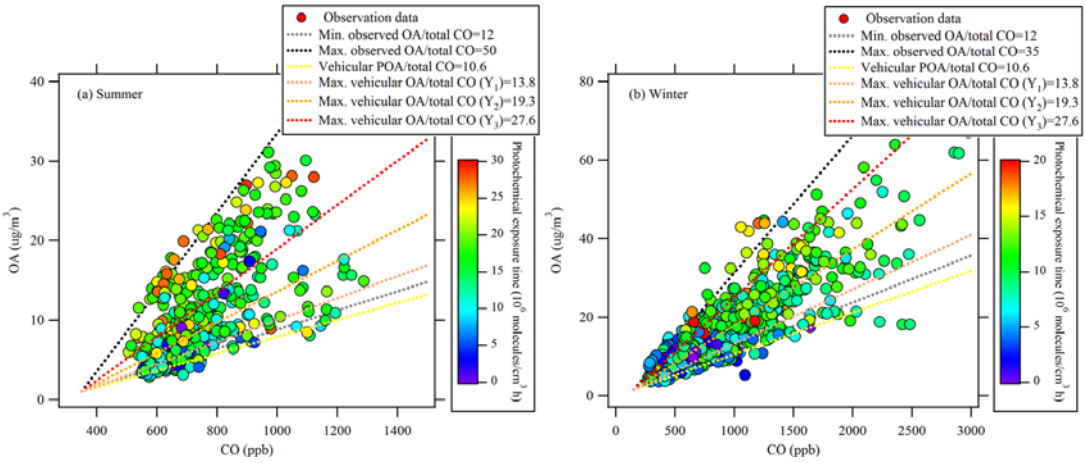

Fig. 6. Relationship of measured OA and CO concentrations color-coded by the photochemical exposure in the summer (a) and winter (b) of 2013 in urban Shanghai according to equation (4). Minimum and maximum ratios of observed OA to CO concentrations are shown by dotted grey and black lines. Vehicular POA/Total CO is shown by dotted yellow line. The minimum and maximum OA formation ratios of vehicle emissions calculated with three different SOA yields of Y1, Y2 and Y3 are shown by the dotted pink, orange and red lines, respectively.

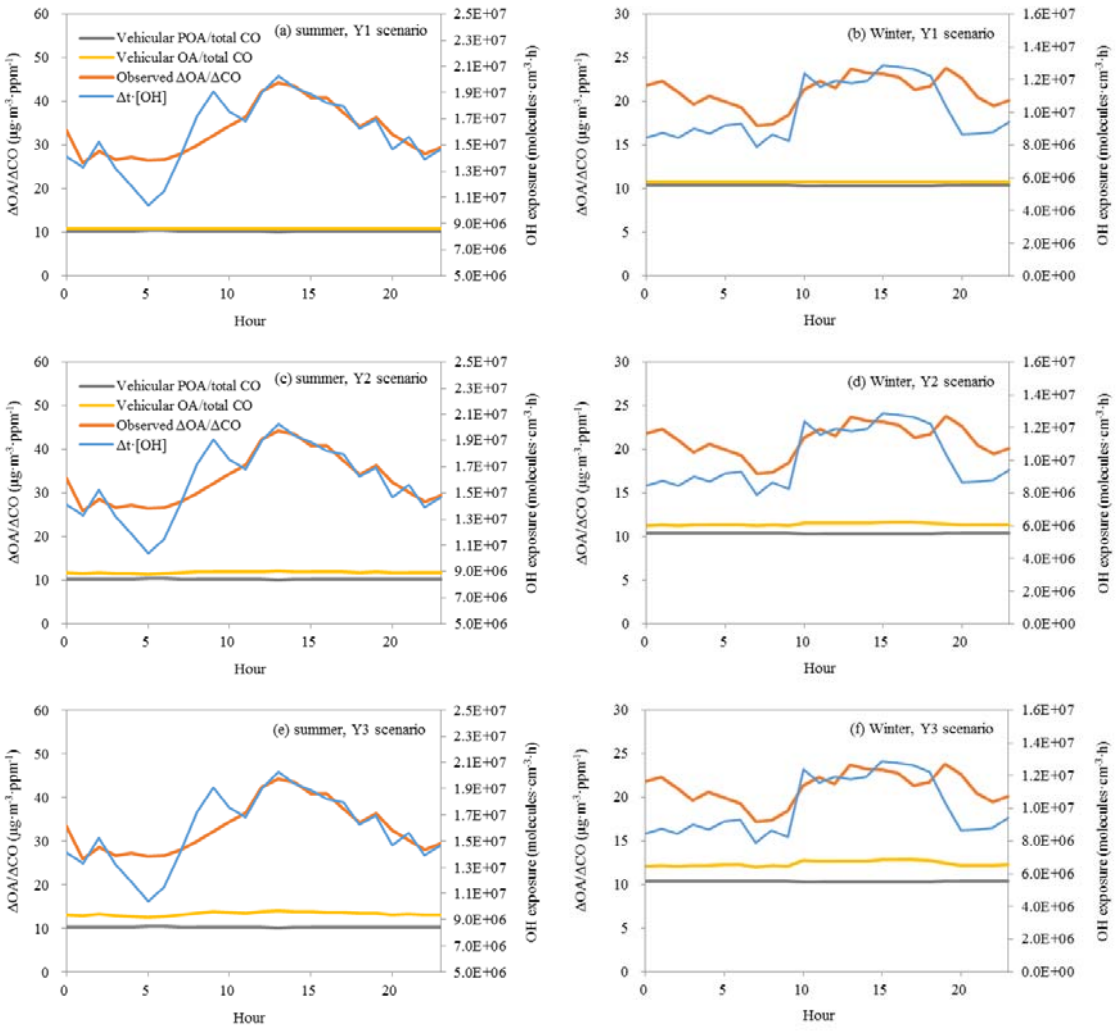

Fig. 7. Diurnal variations of observed ΔOA/ΔCO in the atmosphere (red line), OH exposures (blue line), and the ratios of vehicular POA emission (grey line) and OA formation (orange line) to total CO emissionswith the SOA yields in three scenarios (Y1, Y2 and Y3) in summer and winter in the urban area of Shanghai for the year of 2013.

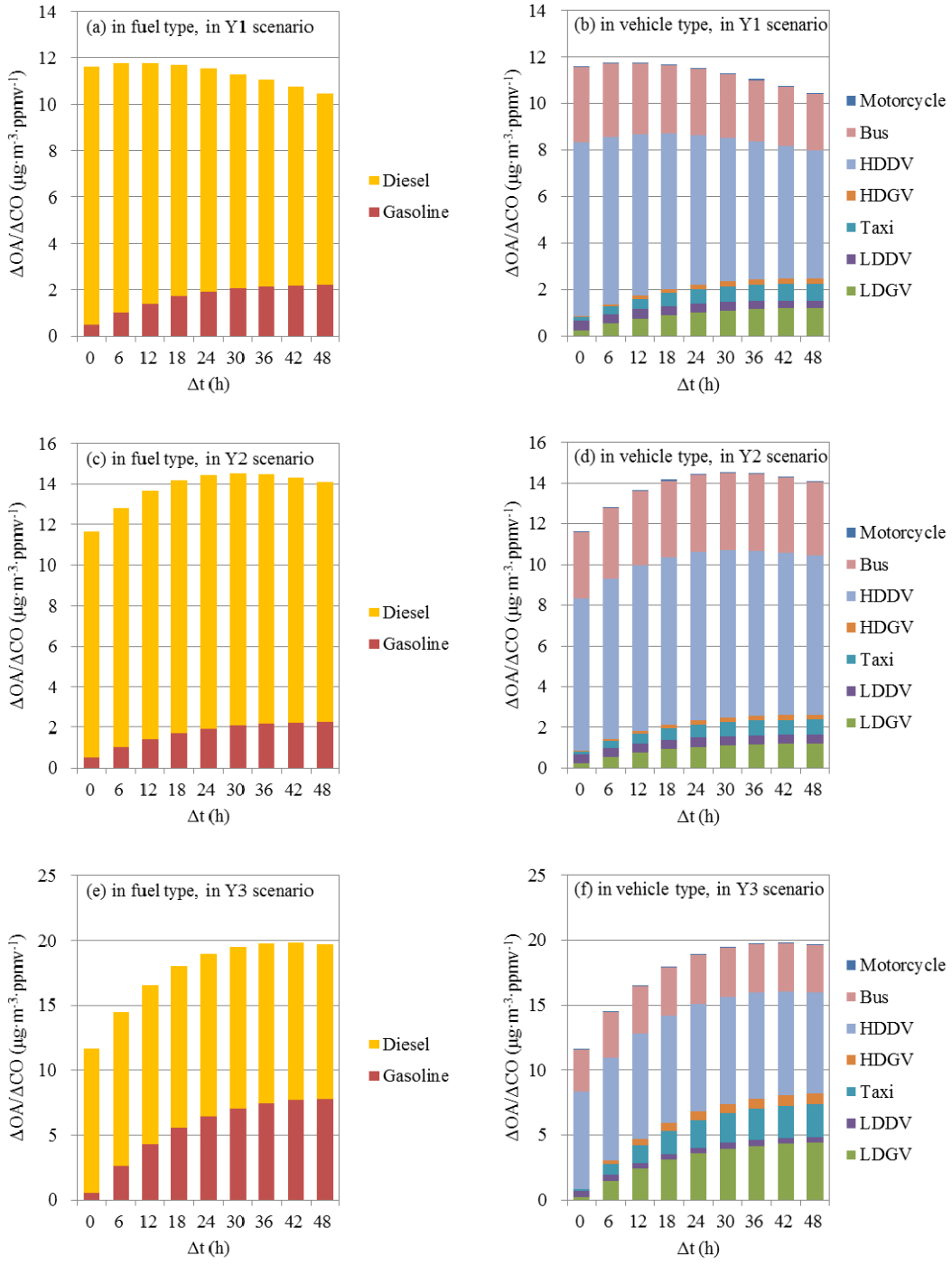

Fig. 8. Contributions of vehicle emissions to OA formation ratios in different vehicle and fuel types in Y1, Y2 and Y3 scenarios with the changes of photochemical ages.